Design and Simulation of a Fluidized Bed Dryer for Saffron Drying with an Approach to Reducing Energy Consumption

Amir Hossein Sharifi, Babak Beheshti[1*], Mohammad Qahdrijani [2]

Received: 2024-10-14 Accepted: 2024-12-11

Abstract

Today, the development of food systems and agricultural goods is often the largest contributor to national economies and plays a key role in achieving sustainable development goals. Meanwhile, food and nutrition are essential to citizens' health, and food preservation specialists are systematically working toward progress in creating a more sustainable system. Saffron is a highly valuable spice extracted from the flower's stigma. Drying is a crucial process in saffron production, as it helps preserve the spice's flavor, aroma, and color. Proper storage helps maintain the quality of saffron over a long period. In this study, the Computational Fluid Dynamics (CFD) method was used to model the saffron experimental Fluidized bed dryer. The behavior of the fluid within the dryer was examined utilizing the computational fluid dynamics and the turbulent flow ε-k as a turbulence model using the Fluent software. The device was simulated at three different air temperatures—60, 65, and 70 °C—and three different air speeds: 1.5, 52.5, and 5.3 m/s. Results of analysis of the coefficient of variance of inlet air temperature and dryer air velocity on humidity with Mean square humidity (20.96) demonstrated that better results are attained when the dryer's air speed is lowered and its input air temperature is raised, or vice versa. Thus, if a dryer is manufactured, it needs to be able to change both the speed and the temperature to reach 10% humidity (wetness-based).

Keywords: Computational Fluid Dynamics (CFD), Fluidized bed dryer, Simulation, Saffron

Introduction

Crocus sativus L. is a perennial herbaceous plant belonging to the Iridaceae family, cultivated in various regions across the globe. Countries such as France, Italy, Spain, Greece, and Turkey are recognized for their saffron production. Significant producers also include Iran, Azerbaijan, as well as large nations like India and China. This plant typically grows to a height of approximately 10–25 cm and is primarily propagated from a corm, a bulbous tuberous structure that regenerates annually. The flower features six tepals, three stamens, and a style that ends in three red-branched stigmas. The spice known as "saffron" is derived from the dried stigmas of *Crocus sativus* L. and is among the most esteemed agricultural products, utilized in

1-Department of Biosystems Engineering, Science and Research branch, Islamic Azad University, Tehran
2-Department of Agricultural mechanization, Science and Research Branch, Islamic Azad University, Tehran, Iran
*The corresponding author email address: beheshti-b@srbiau.ac.ir
Doi: 10.48308/pae.2025.236532.1085

culinary applications to enhance flavor, color, and aroma in various dishes (Alsanie et al., 2022). Saffron possesses several medicinal properties including aphrodisiac, antispasmodic, antimicrobial, antibacterial, antifungal, antiseptic, and anti-inflammatory (Siddique et al, 2020). Saffron plays a pivotal role in maintaining the homeostatic balance and regulating the gut microbiome, thereby contributing to gut health (Singh et al., 2023).

The saffron spice is derived from the dried stigmas of the *Crocus sativus* flower. Its primary applications are in culinary practices, where it is esteemed for its ability to impart color, flavor, and fragrance to various traditional dishes(Bagur et al., 2017).

Yield loss can result from various factors, including poor soil fertility, lack of reliable irrigation, unavailability of high-quality corms for propagation, rodent infestation, and diseases. Additional factors include inadequate post-harvest management, insufficient marketing facilities, adulteration, and the adverse effects of climate change (Cardone et al., 2020).

The post-harvest drying process represents an important step in developing saffron with specific morphological, physical, and chemical characteristics (Masi et al., 2016). The reduction in the commercial quality of saffron can be attributed to improper harvesting methods, inadequate drying processing, exposure to direct sunlight, improper storage, and adulteration (Farag et al., 2020). Saffron is extracted from Crocus sativus L. The stigmas are dried and used as a natural coloring agent or flavoring in cooking (Sarfarazi et al., 2019). In addition to coloring food, it acts as an antioxidant (Kosar et al., 2017) and possesses medicinal properties. The name “saffron” is derived from the Arabic word “ زَعْفَرَان” (zaʿfarān), meaning “yellow,” or the Persian word “زعفران” (zaʿ-farān), which translates to “golden flowers.” The Greeks referred to it as “krokos” (Shahi et al., 2016). Historically, the cultivation and use of saffron have spanned over 3,500 years across various cultures, continents, and civilizations (Zhao et al., 2019). It is believed that the origin of this practice is in the Eastern Mediterranean, from where the cultivation of this plant spread to other parts of the ancient world. Many species of Crocus originate from Crete and the islands of the Aegean Sea, which can be considered the birthplace of saffron. Saffron is one of the most traditional spices and even appears in the frescoes of the Palace of Minoan in Crete. Today, the spice known as “red gold” or “soft gold” (Mzabri et al., 2019; Rocchi et al., 2018).

Saffron, a costly agricultural crop, is essential to the national exports. Without Iran, the world’s annual output of this commodity is just 180 tons, but when it is produced there, it exceeds 200 tons. Iran has not yet established a place for itself in the export of this item, though. Drying is one of the oldest and most common methods for preventing the spoilage of harvested products and allows for longer storage. Since ancient times, humans have paid attention to drying agricultural and food products.

Various methods have been used for drying. Choosing the type of dryer is one of the most important challenges. The drying process is one of the most energy-intensive processes in various industries. Implementing this process with high thermal efficiency while maintaining the quality of the material being dried is of significant importance. This process is one of the most practical operational units used in a wide range of industrial applications, from food to pharmaceuticals. It requires a significant amount of energy, primarily due to the high latent heat of vaporization of water and the relatively low thermal efficiency of dryers. Improving thermal efficiency in the drying process is of great importance due to the high cost of energy and environmental issues. Therefore, finding methods to conserve energy consumption is of paramount importance. Among the various types of dryers, fluidized bed dryers hold a special significance and importance. The main advantages of this type of dryer include excellent mass and heat transfer conditions due to good contact between the particles and the drying gas, uniform mixing of materials within the drying chamber, uniform temperature and moisture distribution within the bed, high drying capacity, rapid operation, and low cost (Mazidi et al., 2019; Masters, 1985; Keey, 1992; Mujumdar, 1995; Sarreshtehdari et al., 2014; Bahu, 1991). The development of modern dryers allows for not only the acceleration of drying operations but also the minimization of waste and energy consumption to the lowest possible level (Kelikanlou et al., 2018). Using fluidized bed dryers allows for the uniform drying of agricultural products in a shorter time compared to conventional dryers. In fluidized bed dryers, products are lifted slightly above their fixed bed due to air pressure, allowing for better moisture exchange with the surrounding air. As a result, the product dries rapidly and uniformly in a short period (Boorker et al., 2006).

A key contributing factor is the careless and unregulated drying of saffron stigma. One of the key processes in producing this product is drying the saffron. Saffron quality will significantly decline if the drying process is done incorrectly (Azghandi, 2014).

In another method, a one-meter-high metal frame is used, which has three to four tiers spaced twenty centimeters apart and made of mesh, making it portable. By placing a heater (heat source) next to the frame and using a ceiling or tabletop fan on a low speed, saffron is dried quickly (Taslemi et al., 2006). On the other hand, due to the problems arising from synthetic packaging on the environment, there is increasing attention to biodegradable food packaging (Maghsoudlou and Razavi, 2016).

The research indicates that incorrect drying of saffron stigmas is the primary cause of quality degradation, hence the drying step of the saffron production cycle is regarded as very important (Brooker et al., 2001).

There is usually one drying phase in industrial operations. Materials can be dried using a variety of techniques, each with unique properties (Mowla and Hatamipour, 2002). Fluidized bed dryers are commonly employed in the drying of several foods because of their high rate of heat and mass transfer, rapid drying speed, and thermal efficiency. The chemical, metallurgical, and pharmaceutical sectors have several uses for fluidized bed dryers (Bialobrzewski et al., 2008).

The conventional procedure involves removing the stigma from the flower and placing it in a clean, dry, warm chamber away from the sun to dry gradually over two to five days. The quality of saffron increases with a shorter drying period. This process may lead to the development and proliferation of microbes, a rise in pollution, and a decrease in coloring power because of the prolonged drying period's effect on enzyme activity.

Another solution involves the use of four one-meter-tall metal bases made of moveable net material and has floors (three to four floors) spaced twenty centimeters apart. They swiftly dry saffron by utilizing a desktop or ceiling fan and putting a heater (heat source) near the stool with high heat (Taslimi et al., 2015).

In an alternative framework, the effectiveness of this method relies on the formation of ice crystals within the stigma tissue. This process employs a freeze dryer. Initially, the product is subjected to a temperature of -18 ºC for a duration of 20 hours, followed by exposure to a temperature of -13 ºC and a pressure of 15 sigma mm Hg, which approximates a vacuum, for a period of 12 hours.

The fast rate of cooling and low temperature in the macroscopic stage cause ice crystals to grow in extremely tiny shapes, preventing tissue injury during freezing and sublimation. Subsequently, subjecting it to a temperature and pressure that is closer to zero, which causes ice crystals to sublimate, the majority of the water in the sample's tissue is eliminated. Compared to the conventional approach (shade-sun), the saffron generated by this process contains more picrocrocin (taste) and safranal (fragrance), but the stigma is fresher and tends to be orange. Compared to the conventional approach, this method of drying saffron yields a reduced amount of crocin (Atefi et al., 2014).

An apparatus was constructed and the electric method of drying saffron was employed for the first time in a study conducted in Afghanistan. Using this apparatus, saffron can be dried in less than an hour and the humidity can be precisely controlled (12 to 14 percent). One drawback of this method is the device's limited capacity, which entirely overshadows its industrial use (Mazloumi et al., 2017).

Infrared dryers were employed in a different design. By producing heat inside the product and concentrating it in areas with higher moisture content, an infrared light induces the moisture to move from those areas toward the outer layers of the product by raising the vapor pressure. Thus, it appears that the problems related to the drying of the saffron's surface layer will be lessened when using this method of drying saffron. It is anticipated that this will shorten the drying period and lessen pulverization and breakage brought on by tensile stress. According to early research, the amount of time needed to dry materials using infrared radiation reduces as the intensity of the radiation increases. However, biological materials break when exposed to infrared radiation for an extended time (Mazloumi et al., 2017).

The current study aims to model the fluidized bed drier and assess its effectiveness at various drying temperatures, speeds, and periods to obtain the desired moisture content of 10% saffron (based on moisture).

Materials and methods

The schematic of the experimental device is presented in Figure 1. The drier cylinder chamber, which was duplicated in this research, represented the most significant element of the apparatus under investigation. The cylindrical configuration of the dryer was utilized as the geometry for the chamber, and both the geometry and network were developed using Gambit software.

where v and ρ represent the speed and density of the fluid, respectively. The conservation of momentum is as follows:

$$\frac{\partial}{\partial t}(\rho\vec{v}) + \nabla_1(\rho\vec{v}) = -\nabla p + \nabla_1(\bar{\tau}) + \rho\vec{g} \quad (2)$$

where $\rho\vec{g}, \bar{\tau}$, p and indicate the gravity field force, stress tensor and static pressure, respectively. The stress tensor is defined as follows:

Using Fluent software, the dryer cylinder was simulated to achieve the required humidity of 10% (based on moisture) after being designed using Gambit software.

Taking into account that the saffron flower, petal, and stigma have maximum speeds of 1.5, 2.5, and 3.5 m/s, respectively (Nemati, et al., 2020), the stigma, petal, and blossom speeds of saffron are considered while determining the speed of the air entering the dryer (Table 1).

The equations governing the problem are as follows. Conservation of mass equation or continuity equation:

$$\frac{\partial \rho}{\partial t} + \nabla_1 \alpha(\vec{v}) = 0 \quad (1)$$

$$\bar{\bar{\tau}} = \mu\left[(\nabla\vec{v} + \nabla\vec{v}^{T}) - \frac{2}{3}\nabla.\vec{v}I\right] \quad (3)$$

where μ and I express the dynamic viscosity and the unit tensor, and the second part on the right side of the equation represents the impact of volume expansion. The energy

$$\frac{\partial}{\partial t}(\rho E) + \nabla_1\big(\vec{v}(\rho E + \rho)\big) = \nabla_1$$

$$\left[k_{eff}\nabla T - \sum_{i} h_j\vec{J}_j + (\bar{\tau}_{eff}\vec{v})\right] + S_h \quad (4)$$

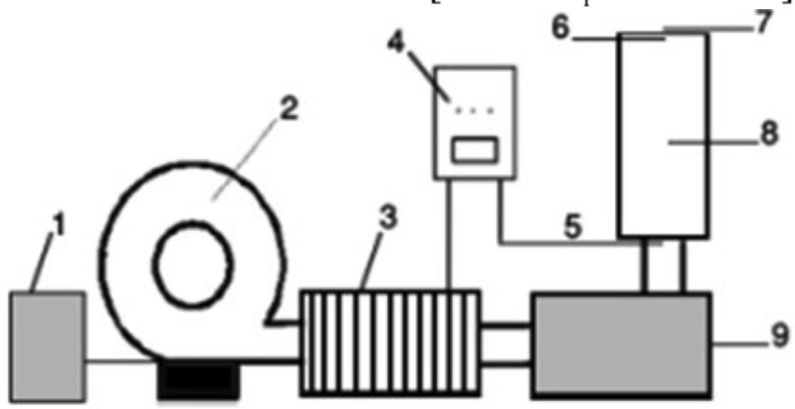

Fig. 1. The schematic of the fluidized bed dryer; 1: Inverter, 2. Fans, 3. Heaters, 4. heater control board, 5 and 6. Thermocouples, 7. Anemometer, 8. Dry fluidizing cylinders, and 9. chambers

Table 1. Drying factors

Inlet air temperature (° C)	60	65	70
Dryer air speed (m/s)	1.5	2.5	3.5

The effective conductivity is denoted by k_{eff} and is equal to $k + k_{\tau}$, , where the turbulence model defines k_{τ}, , the turbulent flow conductivity. J's dispersion flow is denoted by j_j . Equation 4's right-hand side represents the energy transfer resulting from conduction, species diffusion, and viscous dissipation, respectively. The heat from chemical reactions and heat from other sources are included in S_h . Since there was no heat source in this study, S_h was 0. Equation 5 will yield:

$$E = h - \frac{p}{\rho} + \frac{v^2}{2} \tag{5}$$

where the enthalpy for an ideal gas is as follows:

$$h = \sum_j Y_j h_j \tag{6}$$

where the enthalpy for an ideal gas is as follows:

$$h_j = \int_{T_{ref}}^{\tau} C_{vj} dT \tag{7}$$

T_{ref} is 273 degrees Kelvin. The $k - \varepsilon$ model was selected as the turbulence model. The transfer equations for k and ε are as follows:

$$\frac{\partial}{\partial t}(\rho k) + \frac{\partial}{\partial x_j}(\rho k u_j) = \frac{\partial}{\partial x_j}\left[\left(\mu + \frac{\mu_t}{\partial_k}\right)\frac{\partial k}{\partial x_j}\right] + G_k + G_b - \rho\epsilon + Y_M + S_k \tag{8}$$

and

$$\frac{\partial}{\partial t}(\mu\epsilon) + \frac{\partial}{\partial x_j}(\rho k u_j) = \frac{\partial}{\partial x_j}\left[\left(\mu + \frac{\mu_t}{\partial_k}\right)\frac{\partial k}{\partial x_j}\right] + \mu C_2 S_2 - \mu C_2 \frac{\varepsilon^2}{k + \sqrt{v\varepsilon}} + C_{12}\frac{\varepsilon}{k} C_{32} G_k + S_\varepsilon \tag{9}$$

where

$$C_1 = max\left[0.43, \frac{\eta}{\eta + 5}\right]$$

$$\eta = s\frac{k}{\varepsilon}$$

$$s = \sqrt{2S_{ij}S_{ij}}$$

In the equations mentioned above, the kinetic energy produced by turbulence as a result of the mean velocity gradient is expressed as G_k.

The buoyancy force produces kinetic energy turbulence, or G_b.

The contribution of variable expansion in compressible turbulence to the total dissipation rate is denoted by Y_M . The fixed values $C_2 = 1.9$ and $C_{1\varepsilon} = 1.44$ serve as a foundation for verifying that the implemented model is appropriate for the standard flow. In this study, the source terms σ_k and σ_ε were regarded as zero. The constant $C_{1\varepsilon}$ indicates the extent to which the buoyancy force influences ε.

$$C_{1\varepsilon} = tanh\left|\frac{v}{u}\right| \tag{10}$$

where v and u represent the airflow velocity component in the direction parallel to the gravity vector and the flow velocity component in the direction perpendicular to the gravity vector, respectively.

An essential tool for thermal system design and optimization is thermodynamic analysis. The amount of energy used in the fluidization chamber of the wet material drier is directly correlated with the energy consumption ratio, which is the percentage of energy used compared to the usable energy provided by the heater. As a result, the objective function for system optimization was the energy consumption ratio, which is a suitable dimensionless expression. The first rule of thermodynamics was used to compute energy consumption (Tasirin et al., 2007):

$$E_u = m_{da}(h_{dai} - h_{dao})$$

where h_{dai} and h_{dao} indicate the inlet and outlet air enthalpy of the dryer, and the air mass flow m_{da} was calculated as be-

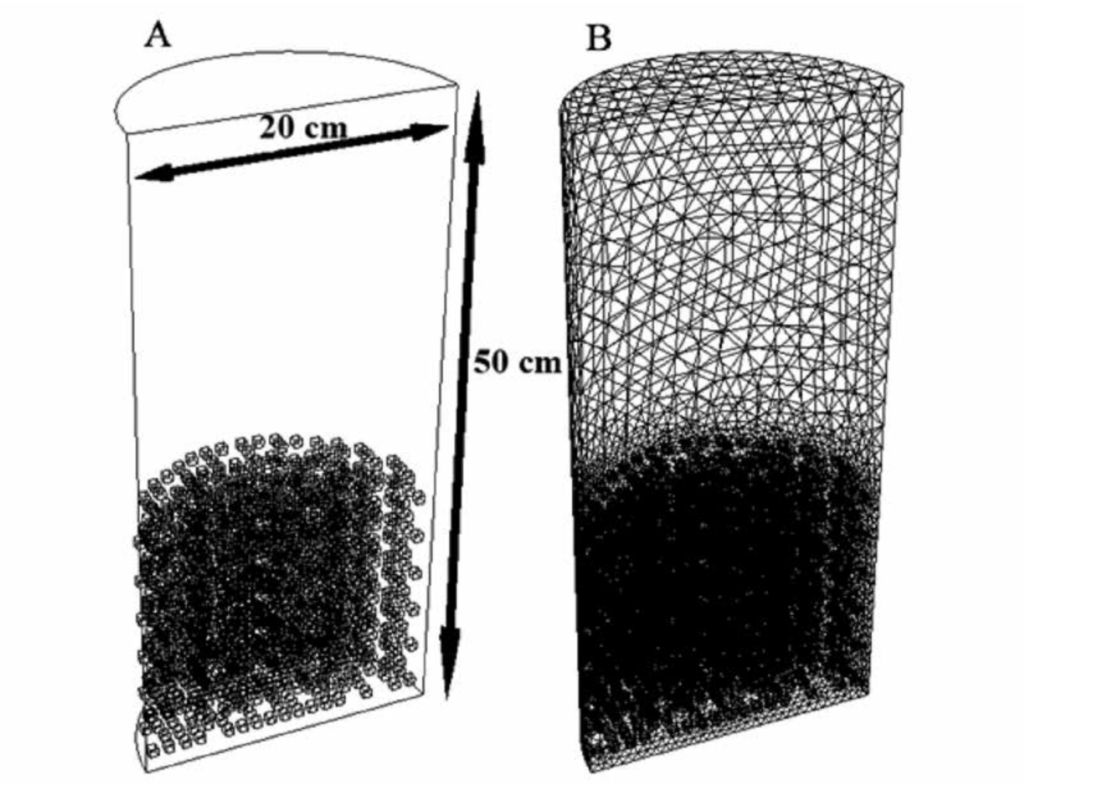

Fig. 2. A) The general plot of the used geometry, bed depth, and size of saffron, (B) meshing by size function

low (Ceylan et al., 2007, Aghbashlo et al., 2008):

$$m_{da} = \rho_{\alpha} v_{\alpha} A_{dc}$$

where v_{α} is the air speed and A_{dc} indicate the dryer chamber surface area. In addition, the enthalpy of drying air can be calculated as below (Corzo et al., 2008):

$$h_{da} = C_{pda}(T - T_{\infty}) + h_{fg}w$$

where T and T_{∞} express the dryer temperature and ambient temperature. C_{pda} , which is the specific heat of inlet and outlet air, was calculated as follows (Corzo et al., 2008):

$$C_{pda} = 1.004 + 1.88w$$

To convert the relative humidity to air humidity ratio, this equation can be applied (Aghbashlo, 2008):

$$w = 0.622 \frac{\varphi P_{vs}}{P - P_{vs}}$$

where φ, P and P_{vs} express the relative humidity of the air, atmospheric pressure, and saturation pressure, respectively.

The humidity ratio of the outlet air was calculated as follows (Akpinar, 2004):

$$w_{dao} = w_{dai} \Big|_{h_{da}}^{DR}$$

$$DR = \frac{W_t - W_{t+\Delta t}}{\Delta t}$$

where W represents the saffron weight (Corzo et al., 2008).

Results and discussion:

Figure 2 displays the problem's geometry as well as the simulation's meshing. Saffron flowers are arranged haphazardly throughout the bed's height (Figure 2).

The most crucial factor that can be observed at any location inside the dryer chamber to determine energy consumption at those loca-

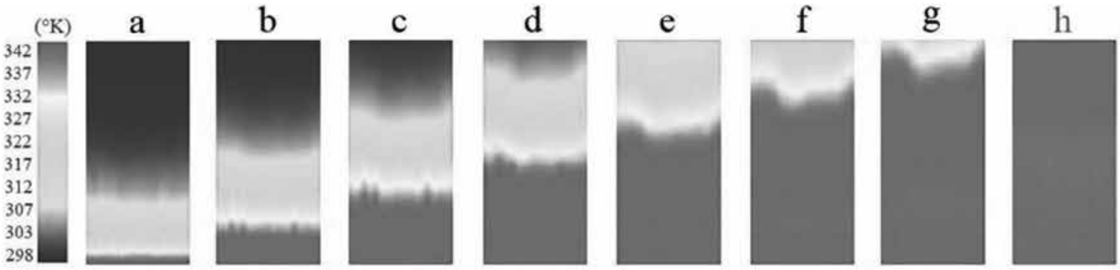

Fig. 3. The total temperature contour at the depth of the bed and inlet temperature of 70°C in time intervals of 5 to 40 minutes

Fig. 4. Division of the dryer chamber into five plates

tions is temperature, as shown by equations 14 and 16. The dryer chamber's temperature contours at various intervals are depicted in Figure 3. Heat transfer from the air to the saffron flowers causes the air temperature at the top of the dryer's cylindrical chamber to be lower than the air temperature at the chamber's bottom. The cylinder's overall temperature was nearly equal to the air inlet temperature at the end of the operation since all simulations were run until stable circumstances were reached.

The height of the dryer chamber was split into many levels (Figure 4) to provide a more precise analysis of the temperature distribution along the cylinder. The temperature was then calculated in each layer. The temperature variations related to time and screen location are depicted in Figure 5. The temperature of the first plate on the dryer chamber floor is the same as the temperature of the inlet air in the first time, as shown in Figure 5. As the height of the plate increased along the drying chamber, the temperature of the plates reduced until it reached the same level as the surrounding air at the top of the chamber. Gradually, the temperature of the top plates rose above the surrounding air and eventually reached a stable condition at the end of the operation, with the lower plates' temperature matching that of the inlet air.

The weight of the material divided by the chamber's cross-sectional area represented the pressure drop of the bed under minimal fluidization circumstances. In other words, the weight of the materials is balanced by the frictional force between them and the air. The fluidized bed around the saffron flower in Figure 5 illustrates how the air viscosity caused the boundary layer at the flower's upper surface to thicken before it split from the plate. When the boundary layer separated, it produced turbulent vortices where energy was lost and the material was subjected to an upward drag force. The combined force exerted on the material is the result of airflow drag on mud surfaces and viscous drag. Figure (5. a) depicts turbulent vortices above a saffron flower, as well as the air velocity and viscous drag vectors around it in a fluidized bed. Figure (5. b) displays the contour of pressure. The graphic illustrates how the formation of vortices causes a pressure drop along the saffron height.

Given that the objective of this research is to achieve the optimal humidity for drying saffron and that the humidity standard is

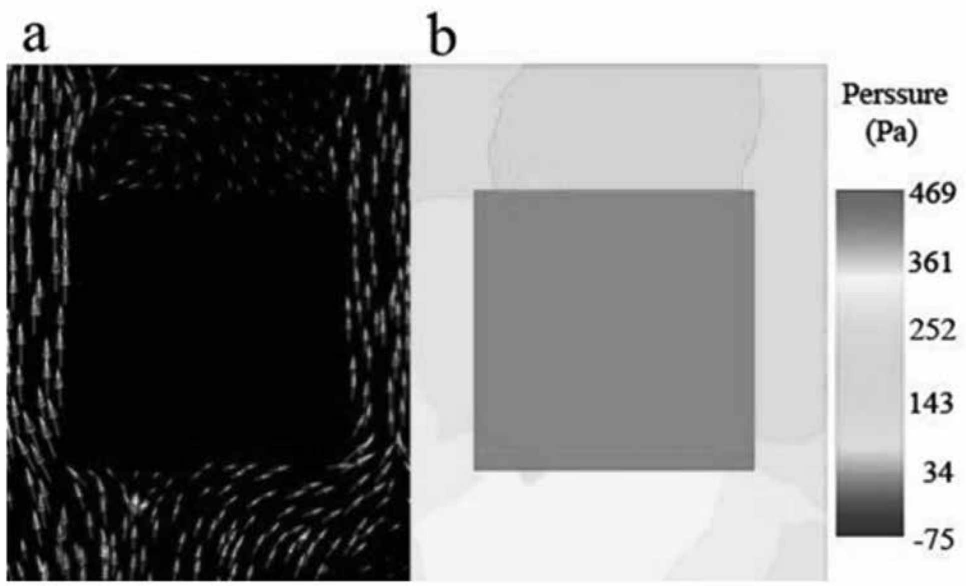

Fig. 6. (a). The total pressure contour (b) Velocity vectors around a saffron flower in a fluidized bed dryer

Table 2. Variance factor of inlet air temperature and dryer air speed on humidity

Changes source	df	Mean square humidity
Inlet air temperature (factor (A)	2	123.11**
Dryer air speed (factor (B)	2	712. 27**
Inlet air temperature * dryer air speed (A*B)	4	20.96**
Error	18	35.37
Coefficient of variation (C.V.)	-	12.17

10% (wetness-based) (national standard of saffron - Iranian standard number 259), the analysis of variance based on Table 2 revealed that the simple and double reciprocal effects in this study exhibit high significance. Consequently, based on the variables of inlet air temperature and drying air speed, and based on the comparison of the average of the three effects, 10% was obtained in six humidity situations (Fig. 7).

In contrast to conventional drying methods, this method eliminates the potential for microorganisms to grow and proliferate, which might lead to increased pollution and a reduction in coloring power due to enzyme activity throughout the extended drying period. Additionally, saffron dried using this process has greater coloration and scent than the saffron frozen method due to its higher concentration of crocin.

Unlike electric dryers, fluidized bed dryers allow for more exact control over the humidity level and have industrial usage. Furthermore, there are no issues with saffron stigmas breaking in these dryers as opposed to infrared dryers because infrared radiation does not expose biological materials to it over an extended period.

Results of analysis of the coefficient of variance of inlet air temperature and dryer air velocity on humidity with Mean square humidity (20.96) demonstrated that better results are attained when the dryer's air speed is lowered and the input air temperature is raised, or vice versa (Table 2).

The results of this study are consistent with the findings of Dandan Chen et al. (2020), who examined the effects of different drying methods on the appearance, microstructure, bioactive compounds, and aromatic compounds of saffron. They also align with the research by Tersa et al. (2021), which investigated the relationship between drying conditions and the formation of volatile com-

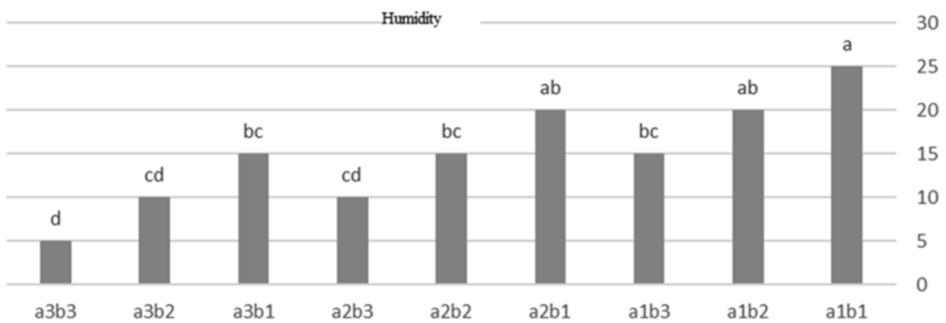

Fig. 7. Comparing the mean interaction effect of inlet air temperature and drying air speed on the moisture content of saffron with 5% LSD

Table 3. The standard drying factor values

Standard humidity (%)	Dryer air speed (m/s)	Inlet air temperature (° C)
10	3.5	65
10	2.5	70

pounds in saffron.

Conclusion

According to the findings, 10% humidity is achieved if the dryer air speed and inlet air temperature are as indicated in Table 3, demonstrating that better results are attained when the dryer air speed and inlet air temperature are greater or lower, respectively. Thus, if the dryer is manufactured, it needs to be able to change its speed and temperature to reach 10% humidity.

Analyzing the findings of the simulation showed that this method can predict the phenomenon of moisture reduction in saffron during the drying process using a fluidized bed dryer.

References

Akpinar, E.K., 2004. Energy and exergy analyses of drying of red pepper slices in a convective type dryer. *International Communications in Heat and Mass Transfer*, *31*(8), pp.1165-1176.

Alsanie, W.F., Alamri, A.S., Abdulaziz, O., Salih, M.M., Alamri, A., Asdaq, S.M.B., Alhomrani, M.H. and Alhomrani, M., 2022. Antidepressant effect of crocin in mice with chronic mild stress. *Molecules*, *27*(17), p.5462.

Atefi, M., Taslimi, A., Shass, M., Mazloumi, M., 2013. Investigating the effects of freeze drying on the quality characteristics of saffron. *Iranian scientific and research quarterly of food science and industry*. D 1. Sh2. pp. 41-49. In Persian

Bahu, R.E., 1991. Energy considerations in dryer design. In *7 th International Drying Symposium in conjunction with the CSI-SA'90 Congress, Prague, Czech, 08/90* (pp. 553-567).

Brooker, D.B., Bakker-Arkema, F.W. and Hall, C.W., 1992. *Drying and storage of grains and oilseeds*. Springer Science & Business Media.

Cardone, L., Castronuovo, D., Perniola, M., Cicco, N. and Candido, V., 2020. Saffron (*Crocus sativus* L.), the king of spices: An overview. *Scientia Horticulturae*, *272*, p.109560. doi: 10.1016/j.scienta.2020.109560.

Chahartaghi, M. and Avatefi Nejad, A.M., 2015. Modeling and analysis of fluidized bed dryer of Bandar Imam Petrochemical Complex for energy and exergy efficiency improvement. *Modares Mechanical Engineering*, *14*(11).

Chen, D., Xing, B., Yi, H., Li, Y., Zheng, B., Wang, Y. and Shao, Q., 2020. Effects of different drying methods on appearance, microstructure, bioactive compounds and aroma compounds of saffron (*Crocus sativus* L.). *Lwt*, *120*, p.108913. doi.org/10.1016/j.lwt.2019.108913.

Farag, M.A., Hegazi, N., Dokhalahy, E. and Khattab, A.R., 2020. Chemometrics-based GC-MS aroma profiling is used to reveal freshness, origin, and roasting indices in saffron spice and its adulteration. *Food chemistry*, *331*, p.127358. doi: 10.1016/j.foodchem.2020.127358.

José Bagur, M., Alonso Salinas, G.L., Jiménez-Monreal, A.M., Chaouqi, S., Llorens, S., Martínez-Tomé, M. and Alonso, G.L., 2017. Saffron: An old medicinal plant and a potential novel functional food. *Molecules*, *23*(1), p.30. doi: 10.3390/molecules23010030.

Keey, R.B., 1991. *Drying of loose and particulate materials*. CRC Press.

Kelikanlou, V., Rahmati, M.H. and Alizadeh, M.R., 2018. Effect of air temperature and flow rate on energy consumption and drying rate of three paddy varieties in fluidized bed dryer. *Iranian Journal of Biosystems Engineering*, *49*(2), pp.161-170. doi: 10.22059/ijbse.2017.142384.664730. In Persian

Kosar, M., Demirci, B., Goger, F., Kara, I. and Baser, K.H.C., 2017. Volatile composition, antioxidant activity, and antioxidant components in saffron cultivated in Turkey. *International journal of food properties*, *20*(sup1), pp.S746-S754. doi: 10.1080/10942912.2017.1311341

Maghsoudlou, Y., razavi, R. (2016). Antioxidant effects of carboxymethyl cellulose edible coatings with antioxidant on the oxidative stability of the edible pine nut. *Food Processing and Preservation Journal*, *8*(1), 67-85. doi: 10.22069/ejfpp.2016.3136. In Persian

Masi, E., Taiti, C., Heimler, D., Vignolini, P., Romani, A. and Mancuso, S., 2016. PTR-TOF-MS and HPLC analysis in the characterization of saffron (*Crocus sativus* L.) from Italy and Iran. *Food chemistry*, *192*, pp.75-81.

Masters, K., 1985. *Spray Drying handbook*, fourth ed., Longman Scientific & Technical, London, pp: 96-110.

Mazidi, M., Taheri Geravand, A., Jaafari S.M., 2019. Simulation, calculation and the possibility of reducing energy consumption in the spray drying process. *Journal of Food Processing and Preservation*, *1*(1): 31-43. In Persian.

Mazloumi, M.T., Taslimi, A., Jamshidi, A., Atefi, M., Javadi, N., Kamili, F., Ahmadian, F., Falahat, H., Chobdar, N., and Hadian, Z., 2017. Comparison of the effects of vacuum, freezing, solar and microwave drying processes with the traditional method on the properties of saffron. *Pejouhandeh, 13*(3), pp. 223-213. In Persian

Mujumdar, A.S. and Zhonghua, W., 2007. Thermal drying technologies—Cost-effective innovation aided by mathematical modeling approach. *Drying technology*, *26*(1), pp.145-153.

Mujumdar, A.S. Impingement drying. In *Handbook of Industrial Drying*, 3rd Ed; Mujumdar, A.S., Ed.; Taylor & Francis: New York, 2006; 385–396.

Mujumdar, A.S. *Research and development in drying*: Recent trends and future prospects. Drying Technology 2004, 22 (1–2), 1–26.

Mujumdar, A.S., 2006. *Handbook of industrial drying*. CRC press.

Mujumdar, A.S., 2006. *Handbook of industrial drying*. CRC press.New York, 2006; pp. 173–202.

Mzabri, I., Addi, M. and Berrichi, A., 2019. Traditional and modern uses of saffron (*Crocus sativus*). *Cosmetics*, *6*(4), p.63. doi: 10.3390/cosmetics6040063.

Nemati, J., Beheshti, B., Barqei, S.A.M., 1400. Design, construction and evaluation of cyclone separator to separate stigma from saffron petals. *Agricultural Mechanization and Systems Research*, *22*(78), pp.37-54. In Persian.

Rocchi, R., Mascini, M., Sergi, M., Compagnone, D., Mastrocola, D. and Pittia, P.,

2018. Crocins pattern in saffron detected by UHPLC-MS/MS as marker of quality, process and traceability. *Food chemistry*, *264*, pp.241-249. doi: 10.1016/j.foodchem.2018.04.111

Sarfarazi, M., Jafari, S.M., Rajabzadeh, G. and Feizi, J., 2019. Development of an environmentally-friendly solvent-free extraction of saffron bioactives using subcritical water. *LWT*, *114*, p.108428. doi: 10.1016/j.lwt.2019.108428.

Shahi, T., Assadpour, E. and Jafari, S.M., 2016. Main chemical compounds and pharmacological activities of stigmas and tepals of 'red gold'; saffron. *Trends in Food Science & Technology*, *58*, pp.69-78. doi: 10.1016/j.tifs.2016.10.010.

Siddique, H.R., Fatma, H. and Khan, M.A., 2020. Medicinal properties of saffron with special reference to cancer—a review of preclinical studies. *Saffron*, pp.233-244.

Singh, G., Brim, H., Haileselassie, Y., Varma, S., Habtezion, A., Rashid, M., Sinha, S.R. and Ashktorab, H., 2023. Microbiomic and Metabolomic Analyses Unveil the Protective Effect of Saffron in a Mouse Colitis Model. *Current Issues in Molecular Biology*, *45*(7), pp.5558-5574.

Taslimi, A. Mazloumi, M. Jamshidi, A. 2015. Comparison of the effects of solar and vacuum drying with traditional methods on the characteristics of saffron. *Scientific Research Quarterly Journal of Food Sciences and Industries of Iran*. D 3, Sh. 10. pp. 9-18. In Persian.

Zhao, M., Wang, B., Xiang, L., Xiong, C., Shi, Y., Wu, L., Meng, X., Dong, G., Xie, Y. and Sun, W., 2019. A novel on-site and visual molecular technique to authenticate saffron (Crocus sativus) and its adulterants based on recombinase polymerase amplification. *Food Control*, *100*, pp.117-121. doi: 10.1016/j.foodcont.2019.01.0111.